

Assembly of Thiometalate-Based $\{\text{Mo}_{16}\}$ and $\{\text{Mo}_{36}\}$ Composite Clusters Combining $[\text{Mo}_2\text{O}_2\text{S}_2]^{2+}$ Cations and Selenite Anions

Hong-Ying Zang, Jia-Jia Chen, De-Liang Long, Leroy Cronin,* and Haralampos N. Miras*

Polyoxometalates (POMs) have been the subject of a large number of studies due to their nanoscale size, versatile architectures and tunable electronic and physical properties,^[1–4] as well as fundamental investigations of self-assembly in supramolecular chemistry.^[5,6] Recent efforts to investigate the polyoxometalate reaction parameter space has led to exciting discoveries of a vast range of building blocks, however attempts to hybridise material families has been limited.^[7] To address this we wondered if the combination of chalcogenides,^[8,9] which are themselves a very interesting class of compounds in composition and structure, could be hybridised with POMs to yield a new family. This is because we envisaged that the marriage of the two distinct families of diverse POM based and the tunable chalcogen(S and Se)-based synthons could give rise to unprecedented architectures and emergence of unique properties.

In order to investigate the potential from the utilization of novel synthons and the interaction of oxothiometalate-based^[10] building block libraries, we demonstrate the effect of the non-conventional heteroanion^[11] on the self-assembly process and the final structural motifs in oxothiometalate chemistry and we report the synthesis, solid state and solution characterization of two novel nanosized selenite-based oxothiometalate materials, namely: $[(\text{CH}_3)_4\text{N}]_{1.5}\text{K}_{5.5}\text{Na}_2[\text{I}_3\text{C}(\text{Mo}^{\text{V}}_2\text{O}_2\text{S}_2)_8(\text{Se}^{\text{IV}}\text{O}_3)_8(\text{OH})_8] \cdot 25\text{H}_2\text{O}$ **1** and $\text{K}_{13}\text{Na}_3[(\text{Mo}^{\text{V}}_2\text{O}_2\text{S}_2)_{12}(\text{SeO}_3)_6(\text{OH})_{26}(\text{Mo}^{\text{V}}_2\text{O}_2\text{S}_2)_6(\text{O})_5(\text{OH})_3(\text{CH}_3\text{CO}_2)] \cdot 50\text{H}_2\text{O}$ **2**. To the best of our knowledge **1** and **2** are the first selenite-based oxothiometalate clusters reported to date. Additionally, the selenite anion exhibits the rare μ_4 -(η , μ , μ) coordination mode. The compounds were characterized in the solid state and in solution by X-ray structural analysis, UV-vis, Flame atomic absorption spectroscopy, FT-IR, TGA and high resolution electrospray ionization mass spectroscopy (ESI-MS). Furthermore, the compounds were studied for their potential application as electrocatalysts for the production of H_2 gas from aqueous media where they found to be active even at

neutral pH conditions. Furthermore, preliminary proton conductivity properties of compound **1** are reported, demonstrating the multifunctional nature of $\{\text{Mo}_{16}\}$ ring making it a promising candidate for the development of alternative conductive membrane materials for fuel cell applications.

According to our previous work in POM systems we demonstrated initially that incorporation of pyramidal geometry^[11] anions direct the self-assembly process towards the formation of architectures which deviate substantially from the archetypes observed so far in POM systems that incorporate tetrahedral anions such as PO_4^{3-} , SO_4^{2-} and AsO_4^{3-} .^[12] Moreover, the non-conventional geometry gives rise to fundamentally novel properties of the isolated materials with potential applications to molecular electronics and functional nano-materials.^[13]

The addition of $\text{Na}_2\text{SeO}_3 \cdot 2\text{H}_2\text{O}$ (0.2 g) in an aqueous 7.4 mL solution of the dimeric $[\text{Mo}_2\text{O}_2\text{S}_2]^{2+}$ (1 M) unit, followed by the adjustment to the solution to pH 5 by the addition of aqueous 2 M NaOH and heating at 60 °C, resulted in the formation of a dark red solution which yielded crystals of **1** after two weeks. Alternatively, the addition of increased amount of Na_2SeO_3 (0.347 g) in 7.4 mL solution of the dimeric $[\text{Mo}_2\text{O}_2\text{S}_2]^{2+}$ (1 M) unit and adjustment of the pH to higher value (6.8) by dropwise addition of K_2CO_3 (2 M) led to the formation of small red cubic crystals of **2** after three months. Crystallographic studies revealed **1** as $[\text{N}(\text{CH}_3)_4]_{1.5}\text{K}_{5.5}\text{Na}_2[\text{I}_3\text{C}(\text{Mo}^{\text{V}}_2\text{O}_2\text{S}_2)_8(\text{Se}^{\text{IV}}\text{O}_3)_8(\text{OH})_8] \cdot 25\text{H}_2\text{O}$ whereby the anion $[\text{I}_3\text{C}(\text{Mo}^{\text{V}}_2\text{O}_2\text{S}_2)_8(\text{Se}^{\text{IV}}\text{O}_3)_8(\text{OH})_8]^{9-}$ **1a** adopts a nano-sized, 1.6 nm, “star”-shaped ring structure, **Figure 1**, which contains sixteen Mo^{V} centers within the main structural unit. Each molybdenum atom exhibits octahedral coordination and is bonded to a terminal oxo group [1.691(9) Å], two μ - S^{2-} ions [2.317(4) Å], one μ -OH bridge [2.101(9) Å] and two μ -selenite oxygen atoms [2.237(8) Å]. The sixteen Mo^{V} atoms form eight edge shared binuclear units $[\text{Mo}_2^{\text{V}}(\mu\text{-S})_2\text{O}_2]^{2+}$ with a $\text{Mo}^{\text{V}}\text{-Mo}^{\text{V}}$ separation of 2.831(1) Å (single bond). The eight $[\text{Mo}_2^{\text{V}}(\mu\text{-S})_2\text{O}_2]^{2+}$ moieties are connected further to each other by eight selenite ligands and eight hydroxo bridges. All the selenite anions exhibit a μ_4 -(η^2 : η^2 -O:O) bonding mode (Figure 1) with Se-O bonds spanning the range 2.105(8) – 2.375(8) Å. Each one of the μ_4 - SeO_3^{2-} bridges three $[\text{Mo}_2^{\text{V}}(\mu\text{-S})_2\text{O}_2]^{2+}$ dimeric moieties where the selenites and the Mo^{V} -dimers are alternating above and below the plane defined by the ring in a cyclic fashion with the lone pair of electrons of the selenium atom pointing towards the centre of the ring. The centre of the ring is occupied by an I_3^- anion which originates from the stage of oxidation with I_2/KI during the preparation of the dimeric $[\text{Mo}_2^{\text{V}}(\mu\text{-S})_2\text{O}_2]^{2+}$ species (see Supporting Information).

The nanosized rings are stacked together in space, forming a columnar architecture, **Figure 2**, where the rings are separated

H.-Y. Zang, J.-J. Chen, Dr. D.-L. Long, Prof. L. Cronin, Dr. H. N. Miras
WestCHEM, School of Chemistry
The University of Glasgow
Glasgow, G12 8QQ, UK
Homepage: <http://www.croninlab.com>,
Tel: (+44) 141-330-5530, Fax: (+44) 141-330-4888
E-mail: lee.cronin@glasgow.ac.uk; harism@chem.gla.ac.uk
J.-J. Chen
Lu Jiayi Building
Department of Chemistry
Xiamen University
Xiamen, 361005, PR China



DOI: 10.1002/adma.201302565

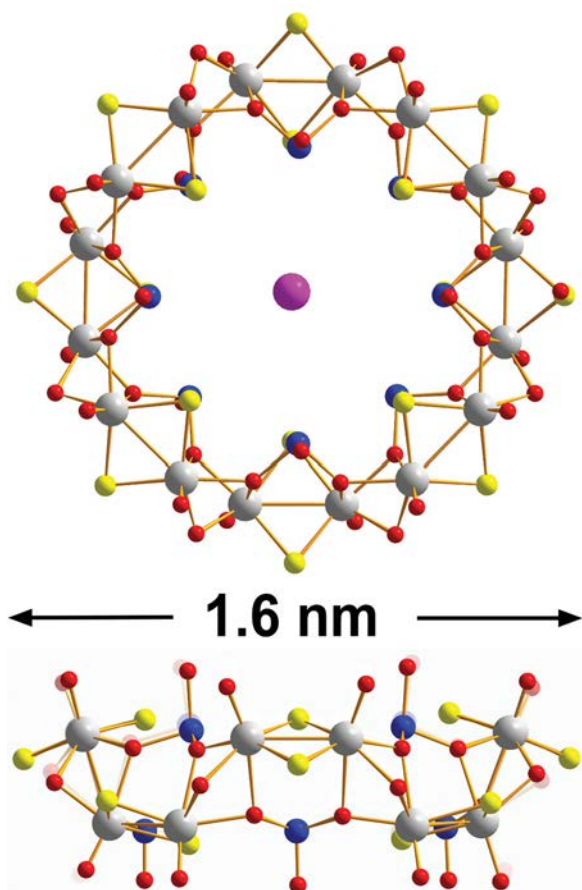


Figure 1. Ball and stick representation of **1** selenite-based oxothiometalate ring. Colour code: Mo: light grey; Se: blue; S: yellow; O: red; I: pink. Counter ions and protons are omitted for clarity.

by a distance of ~ 3.5 Å while the adjacent columns of tubes are ~ 2.8 Å apart (closest proximity) and are separated by a layer of charge balancing counterions (Na^+ and K^+). Bond valence sum (BVS) calculations for the terminal and selenite oxygen atoms are >1.7 (non-protonated), while the $\mu\text{-O}$ bridges gave an average value of 1.1 indicative of their monoprotonated

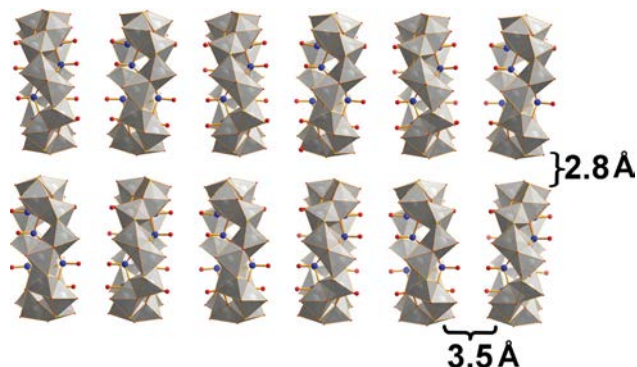


Figure 2. Perspective view along the crystallographic c axis showing a columnar-type framework formation that are partially filled with H_2O molecules and Na^+/K^+ cations. Colour code: Mo: light grey polyhedra; S: small yellow spheres; Se: blue spheres; O: red spheres.

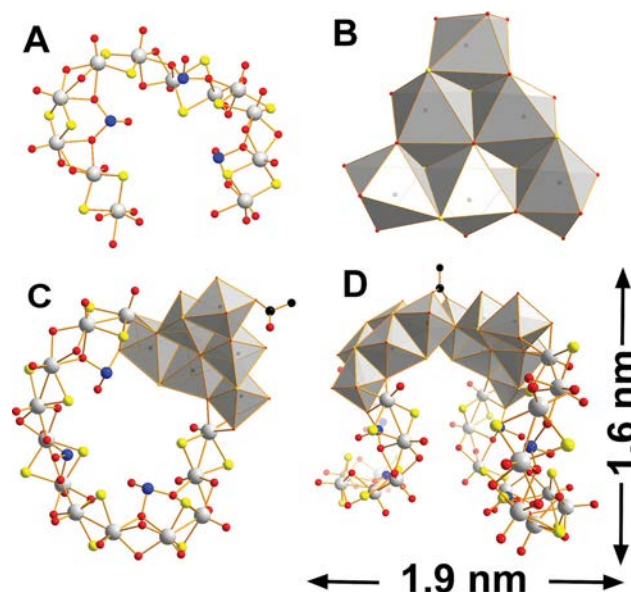


Figure 3. Ball and stick representation of anion's **2a** fragments. A) Horseshoe formation $\{(\text{Mo}^{\text{V}}_2\text{O}_2\text{S}_2)_6(\text{Se}^{\text{IV}}\text{O}_3)_3(\mu\text{-OH})_{13}\}$; B) Hexameric $\{(\text{Mo}^{\text{V}}_2\text{O}_2\text{S}_2)_3(\mu_3\text{-O})_2(\mu_3\text{-OH})_2\}$ unit; C) The distorted ring and the hexameric units are connected together via O-bridges; D) two $\{[(\text{Mo}^{\text{V}}_2\text{O}_2\text{S}_2)_6(\text{Se}^{\text{IV}}\text{O}_3)_3(\mu\text{-OH})_{13}][(\text{Mo}^{\text{V}}_2\text{O}_2\text{S}_2)_3(\mu_3\text{-O})_2(\mu_3\text{-OH})_2]\}$ units are connected further via two O-groups and one CH_3COO^- bridge. Colour code: Mo: light grey polyhedra/spheres; S: yellow; Se: blue; O: red; C: black.

state. In a similar fashion, the BVS calculations for the crystallographically independent molybdenum atoms gave an average value of 5.1.

Compound **2** crystallizes in the monoclinic space group $C2/m$ and exhibits a nanosized (1.6×1.9 nm) anion with the formula $[(\text{Mo}^{\text{V}}_2\text{O}_2\text{S}_2)_{12}(\text{Se}^{\text{IV}}\text{O}_3)_6(\mu\text{-OH})_{26}][(\text{Mo}^{\text{V}}_2\text{O}_2\text{S}_2)_6(\mu_3\text{-O})_5(\mu_3\text{-OH})_3(\text{CH}_3\text{CO}_2)]^{16-}$ **2a**. The anion is constructed by an “open” distorted ring-shaped (horseshoe) formation built-up by six face shared dimeric $[\text{Mo}_2^{\text{V}}(\mu\text{-S})_2\text{O}_2]^{2+}$ moieties, with a $\text{Mo}^{\text{V}}\text{-Mo}^{\text{V}}$ separation of $2.835(3)$ Å (single bond), bridged together via two $\mu\text{-OH}$ groups [$2.15(1)$ Å] and one μ -selenite oxygen atom [$2.29(1)$ Å], **Figure 3A**. The $\text{Mo}^{\text{V}}\text{-Mo}^{\text{V}}$ separation of the neighbouring dimeric $[\text{Mo}_2^{\text{V}}(\mu\text{-S})_2\text{O}_2]^{2+}$ units is $3.228(2)$ Å. All the distances found to be in good agreement with previously reported oxothiometalate species.^[10,11b] The ring formation is completed by a hexameric $\{(\text{Mo}^{\text{V}}_2\text{O}_2\text{S}_2)_3(\mu_3\text{-O})_2(\mu_3\text{-OH})_2\}$ unit, **Figure 3B**, which is connected via three $\mu\text{-OH}$ [$2.17(1)$ Å], two $\mu_3\text{-O}$ groups [$2.13(1)$ Å] and one μ -selenite oxygen atom [$2.18(1)$ Å], **Figure 3C**. Two of the above distorted rings are connected further via the hexameric units with two $\mu_3\text{-O}$ groups and one acetate anion, see **Figure 3D**, creating a complicated architecture with a C_2 symmetry axis passing through the carbon atom of the acetate bridge. To the best of our knowledge, this is the largest selenite-based oxothiometalate species reported so far. BVS calculations in this case for the terminal and selenite oxygen atoms gave values higher than 1.6 (non-protonated), whilst all the $\mu\text{-O}$ bridges gave an average value of 1.1, indicative of their monoprotonated state. Within the hexameric unit, two of the peripheral $\mu_3\text{-O}$ groups gave a value higher than 1.7, while the central and the remaining oxo-group

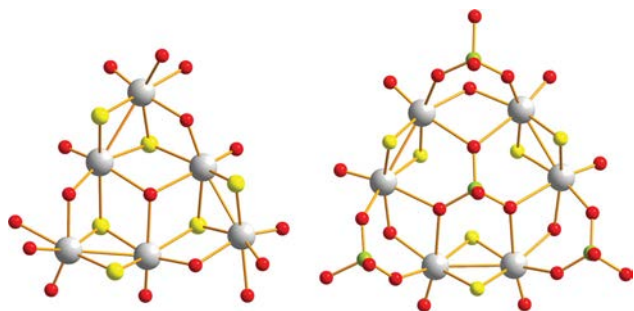


Figure 4. Ball and stick representation of the novel “trapped” hexanuclear moiety (LEFT) and the PO_4^{3-} templated thio-analogue (RIGHT). Colour code: Mo: light grey; S: yellow; P: green; O: red.

were found to be mono-protonated with a BVS value of 0.9. In a similar fashion, the BVS calculations for all the molybdenum atoms gave an average value of 5.1.

It should be noted that the self-assembly process of the molybdenum oxothiometalate system, in the presence of the pyramidal selenite anion at higher pH values, reveals the entrapment of a hexanuclear oxothiometalate species which exhibits an oxo-centered structure. Even though such an hexanuclear oxo- and thio-based species,^[14] templated by phosphate and arsenate anions has been reported before, this is a very rare example^[15] where such a hexanuclear moiety can be formed without a templating tetrahedral anion. Another noteworthy feature of the $\{(\text{Mo}^{\text{V}}_2\text{O}_2\text{S}_2)_3(\mu_3\text{-O})_2(\mu_3\text{-OH})_2\}$ unit is that it represents a compact structure, since the three $[\text{Mo}^{\text{V}}_2\text{O}_2\text{S}_2]^{2+}$ units are shifted in relation to each other, forming a $\sim 70^\circ$ angle, see **Figure 4**. Furthermore, an additional Mo-S bond [2.56(6) Å] is formed between the molybdenum(V) centre of a $[\text{Mo}^{\text{V}}_2\text{O}_2\text{S}_2]^{2+}$ moiety and the sulphur bridge of the neighbouring dimer unit, contributing to the overall integrity/rigidity of the architecture. It is quite intriguing that the “horseshoe” shaped fragment acts as a molecular pincer, which “traps” this unique hexanuclear building unit. This finding demonstrates the potential for the discovery of novel archetypes, and the potential of mixing different sets of building blocks to develop hybrid inorganic clusters further.

The stability and characterization of both compounds were investigated in solution using UV-vis and ESI-MS spectroscopy. These studies showed that their stability is directly related to the pH of the solution rather than the nature of the medium used for the study. For example, compound **1** was found to be stable over a period of 48 h providing that the pH value of the aqueous solution was at least 5. In the case of compound **2** a similar behaviour was observed. At $\text{pH} < 5$, a rapid decomposition was observed. Also, compound **2** showed sufficient stability over a period of 30 hrs in a phosphate buffer medium ($\text{pH} = 7.2$), see SI.

To investigate these two clusters in more detail, we opted to study the clusters further in solution using ESI-MS.^[16] These studies revealed that both the $\{\text{Mo}_{16}\}$ and $\{\text{Mo}_{36}\}$ oxothiometalate species are present in solution. The observation of a series of partially overlapping envelopes is due to the existence of multiple charged states of the same moiety, resulting from the variable number of protons and counterions, which consequently leads to the observation of overlapping isotopic

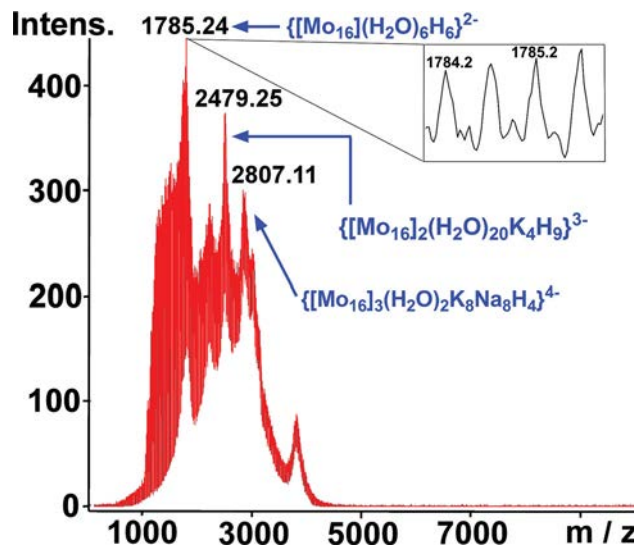


Figure 5. Negative ion mass spectra of **1** in water, showing the discrete $\{\text{Mo}_{16}\}$ ring, $\{[(\text{Mo}^{\text{V}}_2\text{O}_2\text{S}_2)_8(\text{Se}^{\text{IV}}\text{O}_3)_8(\text{OH})_8](\text{H}_2\text{O})_6\text{H}_6\}^{2-}$, the $\{\text{Mo}_{16}\}_2$ dimer, $\{[(\text{Mo}^{\text{V}}_2\text{O}_2\text{S}_2)_8(\text{Se}^{\text{IV}}\text{O}_3)_8(\text{OH})_8]_2(\text{H}_2\text{O})_{20}\text{K}_4\text{H}_9\}^{3-}$ and the $\{\text{Mo}_{16}\}_3$ trimer, $\{[(\text{Mo}^{\text{V}}_2\text{O}_2\text{S}_2)_8(\text{Se}^{\text{IV}}\text{O}_3)_8(\text{OH})_8]_3(\text{H}_2\text{O})_{20}\text{Na}_8\text{K}_8\text{H}_4\}^{4-}$ at $m/z = 1785.24$, 2479.25 and 2807.11 . Inset: expanded distribution envelope of the discrete $\{\text{Mo}_{16}\}$ wheel.

distribution envelopes. This type of behaviour is quite common in aqueous solution studies of POM compounds. In the case of the $\{\text{Mo}_{16}\}^{8-}$ wheel, the observed envelopes centred at $m/z = 1785.2$, 2479.2 and 2807.2 could be assigned unambiguously to -2 , -3 and -4 charged species (**Figure 5**). The doubly charged species can be assigned to the discrete ring with the typical formula $\{[(\text{Mo}^{\text{V}}_2\text{O}_2\text{S}_2)_8(\text{Se}^{\text{IV}}\text{O}_3)_8(\text{OH})_8](\text{H}_2\text{O})_6\text{H}_6\}^{2-}$, while the -3 and -4 charged moieties can be assigned to the “stacked” ring assemblies with formulae, $\{[(\text{Mo}^{\text{V}}_2\text{O}_2\text{S}_2)_8(\text{Se}^{\text{IV}}\text{O}_3)_8(\text{OH})_8]_2(\text{H}_2\text{O})_{20}\text{K}_4\text{H}_9\}^{3-}$ (for the dimer) and $\{[(\text{Mo}^{\text{V}}_2\text{O}_2\text{S}_2)_8(\text{Se}^{\text{IV}}\text{O}_3)_8(\text{OH})_8]_3(\text{H}_2\text{O})_{20}\text{Na}_8\text{K}_8\text{H}_4\}^{4-}$ (for the trimer), in agreement with the crystallographic studies. In the case of the $\{\text{Mo}_{36}\}^{16-}$ species, the spectra appeared to be more complicated due to a higher multitude of overlapping envelopes, arising from the co-existence of different species with the same core structure but different degree of protonation, hydration and number of potassium cations (Figure S11, Supporting Information). Also in this case, ESI-MS studies have been proven to be an important tool in our effort to confirm the integrity, the composition and the intermolecular interactions of such complicated nano-sized systems in solution.

Furthermore, we opted to investigate the potential of our clusters as electrocatalysts for the evolution of H_2 gas from aqueous media. The cyclic voltammograms (CV) were measured in phosphate buffer solution at $\text{pH} 7.2$ for both compounds. An electrocatalytic peak observed in both cases initiating at -500 mV vs. Ag/Ag^+ (-303 mV vs NHE) and -570 mV vs. Ag/Ag^+ (-373 mV vs NHE) for compound **1** and **2** respectively. Relative to the blank buffer solution, the reduction current increased dramatically, which indicates that the compounds exhibit considerable degree of electrocatalytic behaviour (Figure S14). Also, the presence of $[(\text{CH}_3)_4\text{N}]^+/\text{I}_3^-$ ions as hydrogen-bonding chains which interact with water

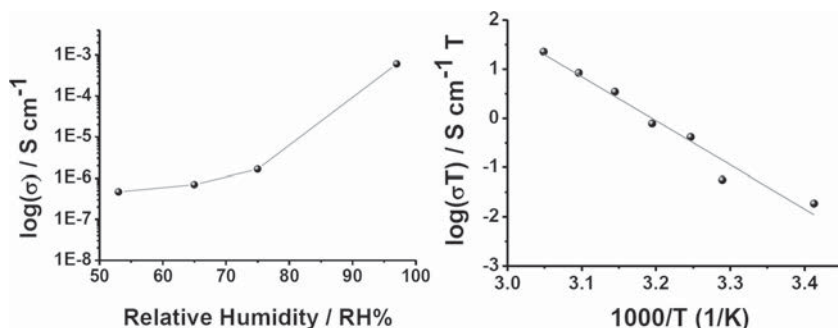


Figure 6. (LEFT) RH dependence of the conductivity (σ) for **1** at 298 K. (RIGHT) Arrhenius-type plot of the conductivity of **1** at various temperatures and under $\sim 97\%$ RH condition.

molecules (proton carriers) creating proton-conducting pathways,^[17,18] makes **1** a promising candidate to be used as proton-conducting solid material with potential applications in fuel cell technology. Moreover, proton-conducting property of materials is mainly influenced by relative humidity, temperature and the content of doped compound. Thus, we employed AC impedance technique for the investigation of the proton conductivity of the solid sample taking into account the above parameters. The humidity dependence of proton conductivities of **1** are shown in **Figure 6**, which are measured at temperatures spanning the range 20 to 55 °C and under relative humidities ranging from 53% to 97% RH. The low-frequency tail observed in the Nyquist plots (Figures S16–S18) is consistent with blocking effects at the electrode, as would be expected for ionic conduction. Analysis on **1** at 97% RH gave a very good conductivity of $1.2 \times 10^{-2} \text{ S cm}^{-1}$ at slightly elevated temperatures (55.0 °C). The activation energy measured was 0.77 eV, indicating a highly efficient “vehicle”-type mechanism^[17] which is reflected by the considerable increase of the conductivity from $6.06 \times 10^{-4} \text{ S cm}^{-1}$ at 20 °C to $1.2 \times 10^{-2} \text{ S cm}^{-1}$ at 55 °C. The observed conductivity value at 55 °C appears to be improved compared with a few MOF-based materials which were recently reported^[18] even though it is still a less efficient proton conductor if we compare with nafion-type membranes.

In conclusion, using non-conventional selenite anions with pyramidal geometry has led to the isolation of the symmetrical 1.6 nm $\{\text{Mo}_{16}\}$ oxothiometalate wheel and the largest oxothiometalate-selenite material reported so far: a 1.9 nm sized $\{\text{Mo}_{36}\}$ species. The isolated compounds represent the highest chalcogen (S + Se) content reported so far: 29.9 and 24.7% for compound **1** and **2**, respectively. The control of the interplay between the pyramidal geometry, the lone pair of electrons and the ionic radius of the selenite anions has been proven to be crucial for the directed self-assembly of the $[\text{Mo}_2\text{O}_2\text{S}_2]^{2+}$ -based building blocks and the engineering of the appropriate curvature, which led to the formation of wheel shaped species. The use of the selenite anion introduced an intriguing diversity to the oxothiometalate system, giving us access to novel libraries of building blocks and, consequently, led to the formation of unprecedented architectures. Moreover, the fruitful utilization of inorganic ligands of pyramidal geometry demonstrates the potential for development of new building-block libraries and novel self-assembly routes, opening up a new dimension for further discoveries and the designing of new chalcogen-hybrid

metal-oxide systems. Finally, both compounds found to be promising electrocatalysts for the proton reduction process even at neutral pH values in aqueous media. Finally, **1** found to be an efficient proton conducting material with a value of $1.2 \times 10^{-2} \text{ S cm}^{-1}$ at slightly elevated temperatures (55 °C). In the future, we will focus our investigations on the exploitation of these novel building block libraries and identify potential correlations between structure and observed properties, towards the designing of functional nanomaterials.

Experimental Section

Synthesis of $[\text{N}(\text{CH}_3)_4]_{1.5}\text{K}_{5.5}\text{Na}_2[\text{I}_3\text{C}(\text{Mo}^{\text{V}}_2\text{O}_2\text{S}_2)_8(\text{Se}^{\text{IV}}\text{O}_3)_8(\text{OH})_8] \cdot 25 \text{H}_2\text{O}$ (1**):** $\text{Na}_2\text{SeO}_3 \cdot 2\text{H}_2\text{O}$ (0.2 g, 0.9 mmol) was added to 7.4 mL of the oxothiometalate dimer $[\text{Mo}_2\text{O}_2\text{S}_2]^{2+}$ solution. The pH subsequently adjusted to pH 5.0 by addition of aqueous 2 M NaOH followed by heating of the mixture at 60 °C for 10 minutes resulting in a dark red solution. The reaction mixture cooled down and filtered. The clear dark red solution left in a 50 mL Erlenmeyer flask at room temperature. Deep red rod shaped crystals formed after one week. Yield: 400 mg, (10%, based on Mo). Elemental analysis for $[(\text{CH}_3)_4\text{N}]_{1.5}\text{K}_{5.5}\text{Na}_2[\text{I}_3\text{C}(\text{Mo}^{\text{V}}_2\text{O}_2\text{S}_2)_8(\text{Se}^{\text{IV}}\text{O}_3)_8(\text{OH})_8] \cdot 10\text{H}_2\text{O}$, $\text{C}_6\text{H}_{46}\text{I}_3\text{K}_{5.5}\text{Mo}_{16}\text{N}_{1.5}\text{Na}_2\text{O}_{58}\text{S}_{16}\text{Se}_8$, MW = 4388 g mol^{-1} , calcd (found): S 11.68, (12.20); C 1.64 (1.20), H 1.05 (1.14), N 0.47 (0.44), Na 1.04, (0.98); K 4.90, (5.17); Mo 35.00 (36.86). FT-IR (KBr): $\tilde{\nu} / \text{cm}^{-1}$ 3404 (br), 1616 (wk), 1105 (wk), 948 (s), 887 (m), 723 (wk), 635 (s), 555 (m), 512 (m), 463 (m).

Synthesis of $\text{K}_{13}\text{Na}_3[(\text{Mo}_2\text{O}_2\text{S}_2)_{12}(\text{SeO}_3)_6(\text{OH})_{26}(\text{Mo}_2\text{O}_2\text{S}_2)_6(\text{O})_5(\text{OH})_3(\text{CH}_3\text{CO}_2)] \cdot 50\text{H}_2\text{O}$ (2**):** $\text{Na}_2\text{SeO}_3 \cdot 2\text{H}_2\text{O}$ (0.3 g, 1.4 mmol) was added to 7.4 mL of the oxothiometalate dimer $[\text{Mo}_2\text{O}_2\text{S}_2]^{2+}$ solution. The pH subsequently adjusted carefully to the pH value of 6.8 by drop wise addition of aqueous 2M K_2CO_3 solution upon stirring. The reaction mixture filtered and the clear dark orange-red solution left in a 50 mL Erlenmeyer flask at room temperature. Small bright-red cubic shaped crystals formed over a 2 month period of time. Yield: 40 mg (1% based on Mo). Elemental analysis for $\text{K}_{13}\text{Na}_3[(\text{Mo}_2\text{O}_2\text{S}_2)_{12}(\text{SeO}_3)_6(\text{OH})_{26}(\text{Mo}_2\text{O}_2\text{S}_2)_6(\text{O})_5(\text{OH})_3(\text{CH}_3\text{CO}_2)] \cdot 50\text{H}_2\text{O}$, $\text{C}_2\text{H}_{132}\text{K}_{13}\text{Mo}_{36}\text{Na}_3\text{O}_{140}\text{S}_{36}\text{Se}_6$, MW = 8056 g mol^{-1} , calcd (found): H 1.63, (1.25); S 14.33, (13.90); Na 0.86, (0.74); K 6.31, (5.96); Mo 42.86 (43.52). FT-IR (KBr) $\tilde{\nu} / \text{cm}^{-1}$ 3409 (br), 1613 (m), 1051 (wk), 943 (s), 887 (m), 730 (m), 667 (s), 601 (m), 509 (m).

Crystal data for 1: $\text{K}_{5.5}\text{Na}_2[(\text{CH}_3)_4\text{N}]_{1.5}[\text{I}_3\text{C}(\text{Mo}^{\text{V}}_2\text{O}_2\text{S}_2)_8(\text{Se}^{\text{IV}}\text{O}_3)_8(\text{OH})_8] \cdot 25\text{H}_2\text{O}$, $\text{C}_6\text{H}_{46}\text{I}_3\text{K}_{5.5}\text{Mo}_{16}\text{N}_{1.5}\text{Na}_2\text{O}_{57}\text{S}_{16}\text{Se}_8$, $M_r = 4659 \text{ g mol}^{-1}$, tetragonal, space group $P42/mbc$, $a = 34.7352(8)$, $c = 19.7947(5)$ Å, $V = 23883(1) \text{ Å}^3$, $\alpha = \beta = \gamma = 90^\circ$, $Z = 8$, $\rho_{\text{calc}} = 2.592 \text{ g cm}^{-3}$, $\lambda(\text{Mo-K}\alpha) = 0.7107 \text{ Å}$, $T = 150(2) \text{ K}$, 183639 reflections measured, 11685 independent reflections ($R_{\text{int}} = 0.1067$), $R_1(\text{final}) = 0.0448$, $wR_2 = 0.1325$, $\text{GoF} = 0.922$.

Crystal data for 2: $\text{K}_{13}\text{Na}_3[(\text{Mo}^{\text{V}}_2\text{O}_2\text{S}_2)_{12}(\text{Se}^{\text{IV}}\text{O}_3)_6(\mu\text{-OH})_{26}] [(\text{M o}^{\text{V}}_2\text{O}_2\text{S}_2)_6(\mu_3\text{-O})_5(\mu_3\text{-OH})_3(\text{C H}_3\text{C O}_2)] \cdot 50 \text{H}_2\text{O}$, $\text{C}_2\text{H}_{132}\text{K}_{13}\text{Mo}_{36}\text{Na}_3\text{O}_{140}\text{S}_{36}\text{Se}_6$, $M_r = 8056 \text{ g mol}^{-1}$, monoclinic, space group $C2/c$, $a = 37.336(3)$, $b = 20.0038(12)$, $c = 32.751(2)$ Å, $V = 23220(3) \text{ Å}^3$, $\beta = 108.325(6)^\circ$, $Z = 4$, $\rho_{\text{calc}} = 3.453 \text{ g cm}^{-3}$, $\lambda(\text{Mo-K}\alpha) = 0.7107 \text{ Å}$, $T = 150(2) \text{ K}$, 124349 reflections measured, 14274 independent reflections ($R_{\text{int}} = 0.1342$), $R_1(\text{final}) = 0.0619$, $wR_2 = 0.1896$, $\text{GoF} = 1.045$. CCDC-919275 and CSD-919275 electronic files contain the supplementary crystallographic data for **1** and **2** respectively. These data can be obtained free of charge from The Cambridge Crystallographic Data Centre via www.ccdc.cam.ac.uk/data_request/cif for compound **1** and from the Fachinformationzentrum Karlsruhe, 76344 Eggenstein-Leopoldshafen, Germany, (fax: +49 7247-808-132, email: crysdata@fiz-karlsruhe.de) for compound **2**.

Supporting Information

Supporting Information is available from the Wiley Online Library or from the author.

Acknowledgements

This work was supported by the ESPRC, the Leverhulme Trust, WestCHEM, the Royal Society/Wolfson Foundation, the University of Glasgow, the Royal Society of Edinburgh and Marie Curie actions.

Received: June 5, 2013

Revised: July 15, 2013

Published online: August 23, 2013

- [1] a) Special Issue on Polyoxometalates. *Chem. Rev.* **1998**, *98*, 1; b) H. N. Miras, J. Yan, D.-L. Long, L. Cronin, *Chem. Soc. Rev.* **2012**, *41*, 7403; c) K. Wassermann, M. H. Dickman, M. T. Pope, *Angew. Chem.* **1997**, *109*, 1513. *Angew. Chem. Int. Ed.* **1997**, *36*, 1445; d) C. L. Hill *J. Mol. Catal. A* **2007**, *262*, 1.
- [2] a) A. Sartorel, M. Carraro, G. Scorrano, B. S. Bassil, M. H. Dickman, B. Keita, L. Nadjjo, U. Kortz, M. Bonchio, *Chem. Eur. J.* **2009**, *15*, 7854; b) Y. Kikukawa, S. Yamaguchi, K. Tsuchida, Y. Nakagawa, K. Uehara, K. Yamaguchi, N. Mizuno, *J. Am. Chem. Soc.* **2008**, *130*, 5472; c) A. M. Khenkin, R. Neumann, *J. Am. Chem. Soc.* **2008**, *130*, 14474.
- [3] a) A. Seko, T. Yamase, K. Yamashita, *J. Inorg. Biochem.* **2009**, *103*, 1061; b) R. Prudent, V. Moucadet, B. Laudet, C. Barette, L. Lafanechere, B. Hasenknopf, J. Li, S. Bareyt, E. Lacote, S. Thorimbert, M. Malacria, P. Gouzerh, C. Cochet, *Chem. Biol.* **2008**, *15*, 683.
- [4] a) A. Müller, P. Kögerler, A. W. M. Dress, *Coord. Chem. Rev.* **2001**, *222*, 193; b) J. Thiel, C. Ritchie, H. N. Miras, C. Streb, S. G. Mitchell, T. Boyd, M. N. C. Ochoa, M. H. Rosnes, J. McIver, D.-L. Long, L. Cronin, *Angew. Chem.* **2010**, *122*, 7138. *Angew. Chem. Int. Ed.* **2010**, *49*, 6984.
- [5] a) Z. H. Peng, *Angew. Chem.* **2004**, *116*, 948–953. *Angew. Chem. Int. Ed.* **2004**, *43*, 930; b) H. D. Zeng, G. R. Newkome, C. L. Hill, *Angew. Chem.* **2000**, *112*, 1841. *Angew. Chem. Int. Ed.* **2000**, *39*, 1772; c) S. G. Mitchell, C. Streb, H. N. Miras, T. Boyd, D.-L. Long, L. Cronin, *Nature Chem.* **2010**, *2*, 308.
- [6] a) H. N. Miras, G. J. T. Cooper, D. L. Long, H. Bögge, A. Müller, C. Streb, L. Cronin, *Science* **2010**, *327*, 72; b) H. N. Miras, J. Yan, D. L. Long, L. Cronin, *Angew. Chem.* **2008**, *120*, 8548. *Angew. Chem. Int. Ed.* **2008**, *47*, 8420; c) H. N. Miras, M. N. C. Ochoa, D. L. Long, L. Cronin, *Chem. Commun.* **2010**, *46*, 8148; d) H. N. Miras, C. J. R. Richmond, D.-L. Long, L. Cronin, *J. Am. Chem. Soc.* **2012**, *134*, 3816.
- [7] D.-L. Long, R. Tsunashima, L. Cronin, *Angew. Chem.* **2010**, *122*, 1780. *Angew. Chem. Int. Ed.* **2010**, *49*, 1736.
- [8] S. Dhingra, M. G. Kanatzidis, *Science* **1992**, *258*, 1769.
- [9] a) H. L. Li, A. Laine, M. O’Keeffe, O. M. Yaghi, *Science* **1999**, *283*, 1145; b) J. He, J. R. Sootsman, L. Xu, S. Girard, J.-C. Zheng, M. G. Kanatzidis, V. P. Dravid, *J. Am. Chem. Soc.* **2011**, *133*, 8786.
- [10] a) E. Cadot, B. Salignac, S. Halut, F. Sécheresse, *Angew. Chem.* **1998**, *110*, 631. *Angew. Chem. Int. Ed.* **1998**, *37*, 611; b) E. Cadot, M.-A. Pilette, J. Marrot, F. Sécheresse, *Angew. Chem.* **2003**, *115*, 2223. *Angew. Chem. Int. Ed.* **2003**, *42*, 2173; d) F. Sécheresse, E. Cadot, C. Simonnet-Jegat, in *Metal Clusters in Chemistry*, (eds.: P. Braunstein, L. A. Oro, P. R. Raithby), Wiley-VCH, Weinheim, Germany, **2008**, *1*, 124.
- [11] a) H. N. Miras, G. I. Chilas, L. Cronin, T. A. Kabanos, *Eur. J. Inorg. Chem.* **2013**, 1620; b) H. N. Miras, J. D. Woollins, A. M. Slawin, R. Raptis, P. Baran, T. A. Kabanos, *Dalton Trans.* **2003**, 3668; c) H. N. Miras, D. J. Stone, E. J. L. McInnes, R. G. Raptis, P. Baran, G. I. Chilas, M. P. Sigalas, T. A. Kabanos, L. Cronin, *Chem. Commun.* **2008**, 4703; d) H. N. Miras, R. G. Raptis, P. Baran, N. Lalioti, M. P. Sigalas, T. A. Kabanos, *Chem. Eur. J.* **2005**, *11*, 2295; e) H. N. Miras, R. G. Raptis, P. Baran, N. Lalioti, A. Harrison, T. A. Kabanos, *C. R. Chim.* **2005**, *8*, 957.
- [12] a) C. du Peloux, A. Dolbecq, P. Mialane, J. Marrot, E. Riviere, F. Sécheresse, *Angew. Chem.* **2001**, *113*, 2521–2523. *Angew. Chem. Int. Ed.* **2001**, *40*, 2455; b) A. K. Cheetham, G. Férey, T. Loiseau, *Angew. Chem.* **1999**, *111*, 3466. *Angew. Chem. Int. Ed.* **1999**, *38*, 3268; c) X. Fang, P. Kögerler, Y. Furukawa, M. Speldrich, M. Luban, *Angew. Chem.* **2011**, *123*, 5318. *Angew. Chem. Int. Ed.* **2011**, *50*, 5212; d) M. Pley, M. S. Wickleder, *Angew. Chem.* **2004**, *116*, 4262. *Angew. Chem. Int. Ed.* **2004**, *43*, 4168.
- [13] a) D.-L. Long, P. Kögerler, L. Cronin, *Angew. Chem.* **2004**, *116*, 1853. *Angew. Chem. Int. Ed.* **2004**, *43*, 1817; b) D.-L. Long, H. Abbas, P. Kögerler, L. Cronin, *Angew. Chem.* **2005**, *117*, 3481. *Angew. Chem. Int. Ed.* **2005**, *44*, 3415; c) J.-P. Zou, G.-C. Guo, S.-P. Guo, Y.-B. Lu, K.-J. Wu, M.-S. Wang, J.-S. Huang, *Dalton Trans.* **2007**, 4854.
- [14] a) E. Cadot, A. Dolbecq, B. Salignac, F. Sécheresse, *Chem. Eur. J.* **1999**, *5*, 2396; b) R. C. Haushalter, F. W. Lai, *Angew. Chem.* **1989**, *101*, 802. *Angew. Chem. Int. Ed.* **1989**, *28*, 743; c) L. A. Mundi, R. C. Haushalter, *Inorg. Chem.* **1992**, *31*, 3050; d) A. Leclaire, C. Biot, H. Rebbah, M. M. Borel, B. Raveau, *J. Mater. Chem.* **1998**, *8*, 439.
- [15] a) H. N. Miras, E. F. Wilson, L. Cronin, *Chem. Commun.* **2009**, 1297; b) E. F. Wilson, H. N. Miras, M. H. Rosnes, L. Cronin, *Angew. Chem.* **2011**, *123*, 3804. *Angew. Chem. Int. Ed.* **2011**, *50*, 3720.
- [16] F. Bannani, S. Floquet, N. Leclerc-Laronze, M. Haouas, F. Taulelle, J. Marrot, P. Kögerler, E. Cadot, *J. Am. Chem. Soc.* **2012**, *134*, 19342.
- [17] a) *Proton Conductors: Solids, Membranes and Gels—Materials and Devices. Series: Chemistry of Solid State Materials*, Ed. 2nd, (Ed: P. Colomban), Cambridge University Press, Cambridge, UK, **1992**; b) P. Colomban, A. Novak, *J. Mol. Struct.* **1988**, *177*, 277; c) N. Agmon, *Chem. Phys. Lett.* **1995**, *244*, 456.
- [18] a) J. M. Taylor, K. W. Dawson, G. K. H. Shimizu, *J. Am. Chem. Soc.* **2013**, *135*, 119; b) A. Shigematsu, T. Yamada, H. Kitagawa, *J. Am. Chem. Soc.* **2011**, *133*, 2034; c) S. Kim, K. W. Dawson, B. S. Gelfand, J. M. Taylor, G. K. H. Shimizu, *J. Am. Chem. Soc.* **2013**, *135*, 963; d) X. Liang, F. Zhang, W. Feng, X. Zou, C. Zhao, H. Na, C. Liu, F. Sun, G. Zhu, *Chem. Sci.* **2013**, *4*, 983.